Nuclear Instruments and Methods in Physics Research A 1065 (2024) 169547

Contents lists available at ScienceDirect

Nuclear Inst. and Methods in Physics Research, A

journal homepage: www.elsevier.com/locate/nima

Early performance of the tracking detector for the FASER experiment

Tomohiro Inada, on behalf of the FASER Collaboration

CERN, CH-1211, Geneva 23, Switzerland

ARTICLE INFO

Keywords:
Silicon microstrip detectors
Tracking detectors
FASER
LHC
Run3

ABSTRACT

FASER is a new experiment aimed at searching for new light weakly-interacting long-lived particles and studying high-energy neutrino interactions in the very forward region of LHC collisions at CERN. The experimental setup is located 480 meters downstream from the ATLAS interaction point, aligned with the beam collision axis. The FASER detector comprises four identical tracker stations made from silicon microstrip detectors. All tracker stations were installed in the LHC complex in 2021. After the commissioning, FASER has been taking physics data since the start of LHC Run 3 in July 2022. In 2022 and 2023, we have successfully collected data from 68 fb^{-1} (inverse femtobarns) of proton–proton collisions at a center-of-mass energy of 13.6 TeV. This paper describes the design, construction and performance with early data of the silicon tracker stations.

Contents

1. Introduction 1
2. The FASER tracking components 2
3. Operation and calibrations in the LHC Run3 2
4. Long-term stability during operation 3
5. Performance 4
6. Future prospects 4
7. Summary 5
Declaration of competing interest 5
Acknowledgments 5
References 5

1. Introduction

The Forward Search Experiment (FASER) at the Large Hadron Collider (LHC) is designed to search for feebly-interacting light particles with masses in the MeV to GeV range, produced in proton–proton collisions [1]. Additionally, a component of FASER, known as FASERν [2], specifically targets the detection of high-energy neutrinos in all three flavors produced in these collisions. The FASER detector is situated in the service tunnel TI12, aligned with the collision axis of the ATLAS experiment. This location, 480 meters from the ATLAS interaction point (IP) as shown in Fig. 1, offers significant advantages, including low background noise from collisions—such as high-energy muons at roughly 1 event per cm^2 per second—and minimal radiation from the LHC, estimated at around 4×10^6 1-MeV neutrons per cm^2 annually. The FASER detector measures approximately 7 meters in length with a sensitive detector area diameter of 20 cm [3] as shown in Fig. 2. Two scintillator veto systems are in place to reject upstream-background charged particles. Two timing and preshower scintillator systems trigger the search for long-lived particles (LLPs) and neutrino. The FASERν emulsion detector, designed to measure neutrinos of all three flavors, is a 1.1-ton apparatus with 730 layers of 1.09 mm tungsten and emulsion. It serves as a part of a tracking detector with submicron spatial resolution, offering 8 interaction lengths, while it does not have a timing resolution and needs to be exchanged every three months to keep reasonable track density. The detector uses a cartesian coordinate system with the z-axis pointing along the light of sight away from ATLAS IP, the y-axis pointing vertically upwards and the x-axis pointing horizontally to the LHC beamline. Permanent dipole magnets of 0.57 T with a 1.5 m decay volume bend charged particles in the y direction, to separate charged particle pairs from LLP decays and facilitate momentum measurement of charged particles.

E-mail address: tomohiro.inada@cern.ch.

https://doi.org/10.1016/j.nima.2024.169547
Received 27 February 2024; Received in revised form 4 June 2024; Accepted 18 June 2024
Available online 24 June 2024

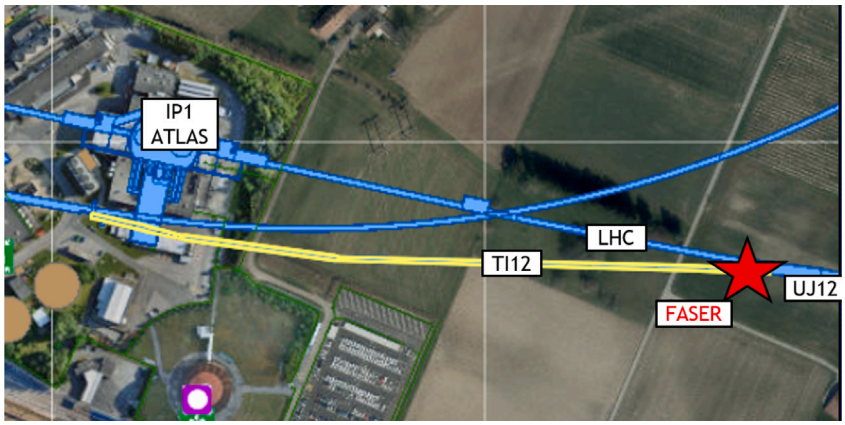

Fig. 1. The FASER detector is located at TI12 tunnel in the LHC, which is 480 m downstream from the ATLAS interaction point [3].

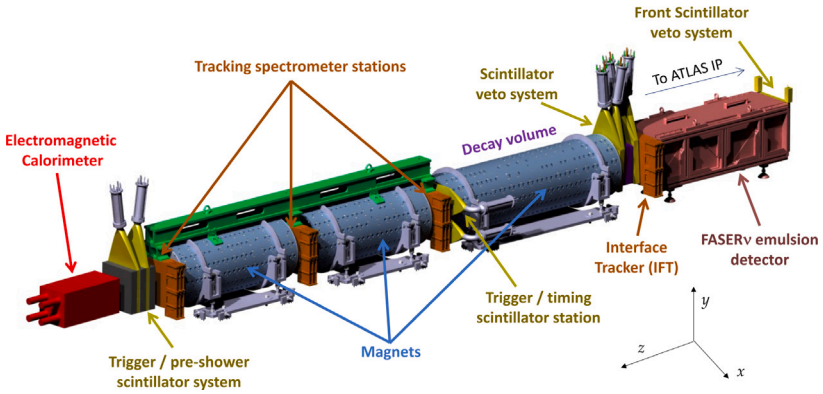

Fig. 2. A schematic view of the FASER detector [3].

Charged particle tracking is primarily performed using four tracker stations, comprising 96 ATLAS semiconductor strip tracker modules (SCT) [4]. The tracker positioned immediately after FASERν, known as the interface tracker (IFT), matches tracks between FASERν and the subsequent spectrometer. This enables the differentiation of charge from neutrino interactions and distinguishes between neutrinos and anti-neutrinos. An electromagnetic calorimeter, located furthest downstream and comprising 4 LHCb outer ECAL modules [5], measures the energies of charged particles.

2. The FASER tracking components

The FASER detector's tracking system comprises four tracker stations. The four tracker stations have identical hardware components. Each of the four stations includes three layers, and each layer is equipped with eight SCT modules. The SCT module is a double-sided silicon microstrip detector with a stereo angle of 40 μrad, which covers an area of 6×12 cm^2 with 768 strips on each side. These strips have a uniform readout pitch of 80 μm and a spatial resolution of approximately 17 μm in the direction perpendicular to the sensor strips (referred to as the precision coordinate) and roughly 580 μm for its resolution parallel to the strips (the non-precision coordinate). The SCT sensor thickness is 285 ± 15 μm. The strips are integrated with ABCD3TA chips [6], a front-end ASIC that provides 128 binary readout channels, each featuring a preamplifier-shaper circuit with a peaking time of about 20 ns. The threshold for each chip is adjustable via an 8-bit DAC. The uniformity of threshold distributions is fine-tuned using the 8-bit DAC for the entire chip and a 4-bit DAC, known as TrimDAC, for each strip. TrimDAC is adjusted by dedicated threshold scans, changing different TrimDAC values, which are called Trim scan. If we cannot adjust a threshold level with any TrimDAC values, we keep those strips as untrimmable cases. Regarding data output, the chip offers a 3-bit binary readout, which is three consecutive time bins to identify hit patterns. The timing is considered to be optimal if the pattern gives 01X (nothing in the first bin, a hit in the second bin and either in the third bin). Details will be discussed in Section 5. For module connectivity, custom-made flexible cables connect a pigtail to a PCB patch panel. Tracker readout occurs through a tracker readout board (TRB), a general-purpose FPGA board. A total of 12 TRBs are present, equating to 1 TRB per tracker plane. 3 m-long Twinac cables transmit data from the patch panels to the TRB. Given the tunnel's low radiation levels, the silicon strip detector operates at room temperature. However, cooling is necessary to dissipate heat—equivalent to 360 W for the entire detector—from the on-detector ASICs. For this purpose, a simple water chiller maintains an internal temperature between 10 and 15 °C. Each station is ventilated with dry air to prevent condensation. A hardware interlock system exists to shut down the tracking stations in the event of cooling or humidity control failure. A custom board for tracker interlock and environmental monitoring sends parameters to the Detector Control System (DCS).

3. Operation and calibrations in the LHC Run3

The FASER detector has been successfully operational since the start of LHC Run 3 in July 2022. We have conducted continuous and predominantly automated data collection at rates up to approximately 1.3 kHz. We have adopted a lightweight operational model without a control room, monitored by a weekly run manager and a monitoring shifter. For fifteen months of operation up to the end of 2023, the total delivered luminosity reached 70.4 fb^{-1}, with the total recorded luminosity at 68.1 fb^{-1}. Tracker calibrations are performed regularly during

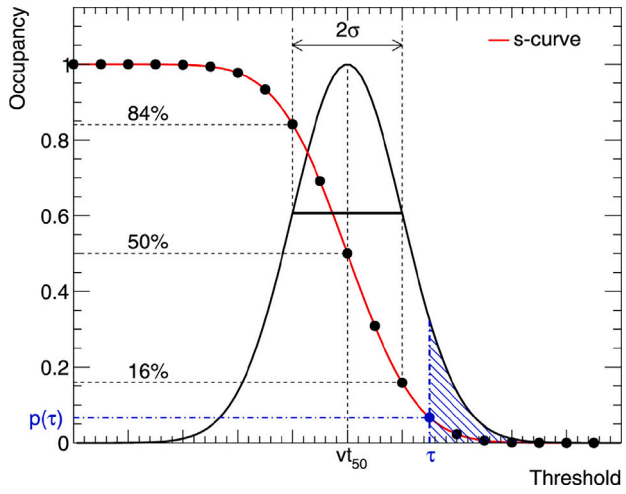

Fig. 3. Illustration of an idealized threshold scan of a single pixel to one constant calibration charge as a function of threshold fitting with an error function (s-curve), overlaid with a Gaussian fit of the derivative of the same curve [7]. The occupancy is the fraction of signals above the threshold (dashed area). The resulting s-curve, essentially a complementary error function, corresponds to the probability that the signal is above the threshold.

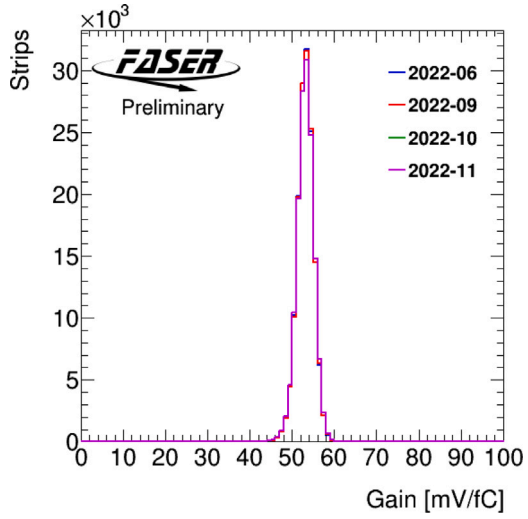

Fig. 4. Comparison of gain distributions of all four tracker stations on a linear scale. These are obtained by regular calibration runs in 2022 during LHC beam downtime. Dead/noisy strips are removed from these plots. We achieve stable operation with more than 99.9% of all strips.

non-beam time with the internal calibration circuit [7]. Most calibration scans rely on threshold scans, as illustrated in Fig. 3. Gain, which is the relationship between comparator voltage and effective threshold charge, is adjustable via a 13-bit bias register that encompasses shaper bias currents and bias current values in the input transistor. By scanning each DAC, gains across all strips are equalized at approximately 54 mv/fC, as depicted in Fig. 4. The equivalent noise charge (ENC), defined as the Gaussian width in Fig. 3, is estimated by injecting a charge of 2 fC into each strip, as shown in Fig. 5. Both the gain and ENC values closely match the expected specifications [6].

4. Long-term stability during operation

Since the start of Run 3, we have conducted continuous calibration runs to monitor tracker parameters, ensuring stable operation and consistent tracker performance. We monitored the gains and ENCs of

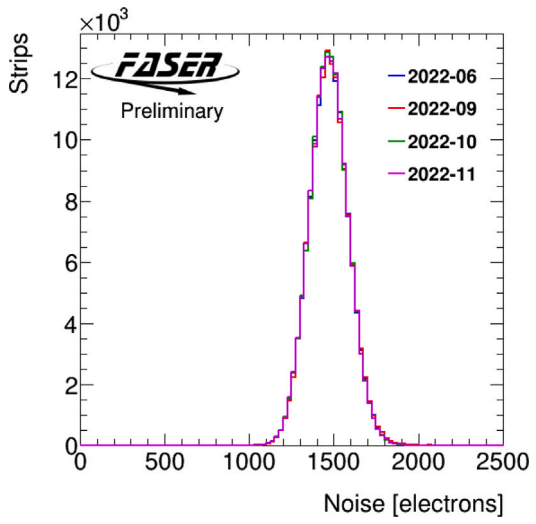

Fig. 5. Comparison of noise (Equivalent Noise Charge, ENC) distributions of all four tracker stations on a linear scale. These are obtained by regular calibration runs in 2022 during LHC beam downtime. Dead/noisy strips are removed from these plots. We achieve stable operation with more than 99.9% of all strips.

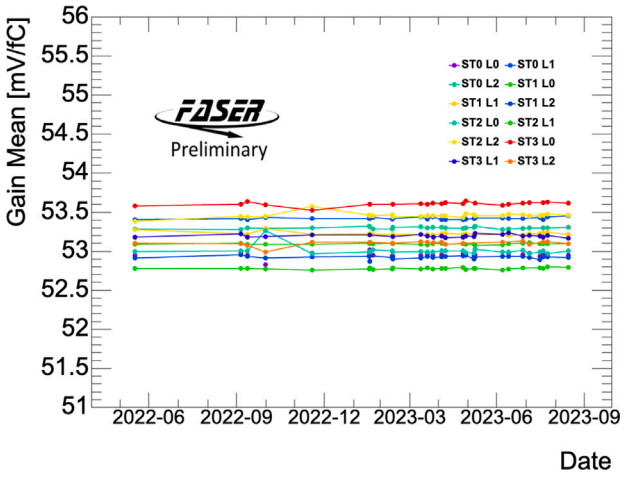

Fig. 6. A history plot of means in gain distributions of each tracker layer fifteen months of operation from June 2022 to September 2023. Each colored line and dot represents one layer and calibration data set.

each layer throughout fifteen months of operation, from June 2022 to September 2023, as depicted in Figs. 6 and 7. These were obtained from regular calibration runs in 2022 and 2023 during periods without LHC beam activity. During calibration runs, it was discovered that several strips were unsuitable for physics analysis. These strips were identified as defective and thus removed from each distribution. Defective strips are defined as follows: (1) dead and noisy strips identified by maskscan, which determines dead and noisy strips by setting a very low or high threshold with charge injection, (2) strips with gains less than 40 mV/fC, (3) strips with ENCs less than 850 electrons, and (4) strips untrimmable across the full range of Trim scans.

The number of defective strips identified by calibration scans over fifteen months operation period has been monitored, as shown in Fig. 8. While most layers have fewer than 100 defective strips, station 3 layer 0 has the highest number (more than 100 strips), mostly clustered within a single chip, a fact that was identified by checking non-linearity with different injection charges. Over 99.7% of the strips are available. Additionally, we have identified the number of noisy strips through offline analysis. The criterion for noisy strips is an occupancy rate

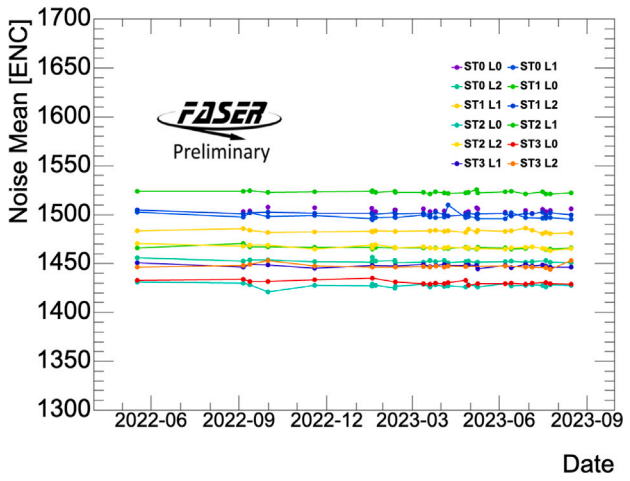

Fig. 7. A history plot of means in noise distributions of each tracker layer over fifteen months of operation from June 2022 to September 2023. Each colored line and dot represents one layer and calibration data set.

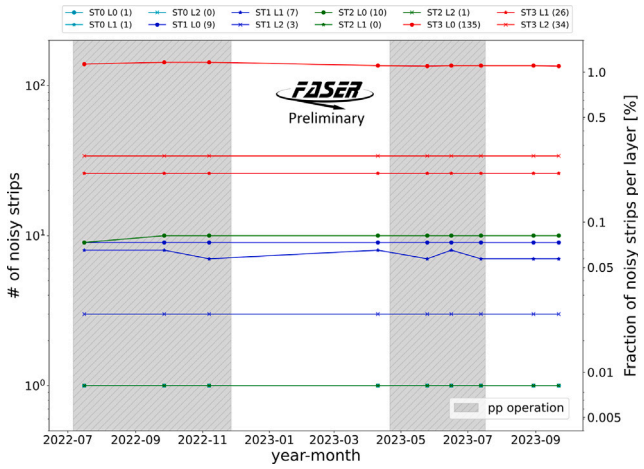

Fig. 9. A history of noisy strips in each layer from June 2022 to September 2023. Each colored line and dot represents one layer and calibration data set, respectively. The number inside the bracket of the legend means the number of noisy strips at the last data point taken in September 2023.

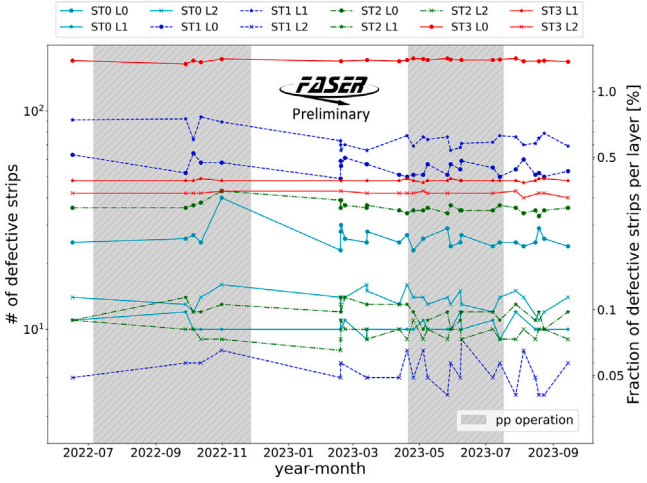

Fig. 8. A history of defective strips in each layer from June 2022 to September 2023. Each colored line and dot represents one layer and calibration data set.

higher than 0.01, exceeding the requirement of less than 5×10^{-4}. Only 0.2% of all strips have been identified as noisy (see Fig. 9), with significant overlap with those labeled as defective. We have maintained stable operation and consistent tracker performance as can be seen from the low and stable number of defective strips, respectively.

5. Performance

We evaluated the tracker performance using early data from 2022 after configuring the trackers' parameters with calibration scans. Initially, we examined a hit map, a distribution of hits on the track for each tracker layer, which demonstrated excellent detector coverage across all layers, except for expected inefficiencies at the edges between modules. To mitigate overlapping inefficiencies, stations are designed with each layer shifted by ±5 mm. Utilizing early LHC fills, which exhibited approximately a 1 kHz muon rate through FASER, which is dominated by muons originating from the ATLAS IP, we conducted timing scans of the trackers. We selected hits with patterns of 010 and 011 (= 01X), which is called edge mode designed for 25 ns LHC bunch spacing and it is with the signal above threshold during bunch crossing, to examine their proportion relative to the total recorded hits. Subsequently, fine timing adjustments were made via clock adjustments on the tracker DAQ boards, selecting the center of the efficiency plateau for optimal timing settings. Furthermore, we assessed hit efficiencies based on varying high voltages (HVs) and threshold levels across tracker layers. For this purpose, we implemented dedicated track reconstruction that blinds one of six strip sensor layers per station, calculating strip efficiency by identifying strips in the blinded sensor layer that align with the track within 500 μm in the y-direction (perpendicular to the magnetic field). Threshold levels were adjusted from 1.0 fC to 3.0 fC and bias HVs from 30 V to 200 V, as illustrated in Fig. 10(a) and (b), achieving a hit efficiency of 99.64 ± 0.10% at a 1.0 fC threshold and 150 V sensor bias, set as the default operational configuration. Though a few chips needed a fine-tuning of threshold level between 1.1 and 1.2 fC to reduce their noise occupancy, we keep the threshold constant for almost all stations.

Offline analysis utilizes tracking performed with ACTS (A Common Tracking Software), implemented in the Calypso framework [8]. The ACTS package [9] enables tracking using the combinatorial Kalman Filter with clusters or space points on the tracker layer, as well as resolving ambiguities between true track seeds and noise. Our event data model closely mirrors that of ATLAS, as Calypso is also based on the Athena software framework used by ATLAS. To verify the effectiveness of our tracking algorithm and to achieve the expected resolution, we conducted the initial alignment using collision data, focusing on three stations, excluding the IFT. Given that this was the first data alignment, the alignment algorithm was designed to be both simple and robust. Consequently, we employed an iterative local chi-square alignment algorithm, which iteratively adjusts one masked layer at a time to identify alignment constants that minimize the chi-square from track fitting. We selected only high-quality tracks, characterized by high momentum ($P_z > 300$ GeV) and a significant number of clusters (total > 14), for validation between data and MC. Concerning the degrees of freedom for alignment constants, we focused on two out of six, Y translation and Z rotation, due to the superior precision on the Y-axis (perpendicular) compared to the X-axis (horizontal), significantly improving track parameters and residuals. Ultimately, we achieved a reasonable residual value of approximately 29 μm, demonstrating good concordance between data and MC, as illustrated in Fig. 11.

6. Future prospects

We plan to enhance the alignment algorithm to enable global alignment of all trackers using the millepede-II algorithm [10], and also plan to develop track matching between the trackers and the FASERν

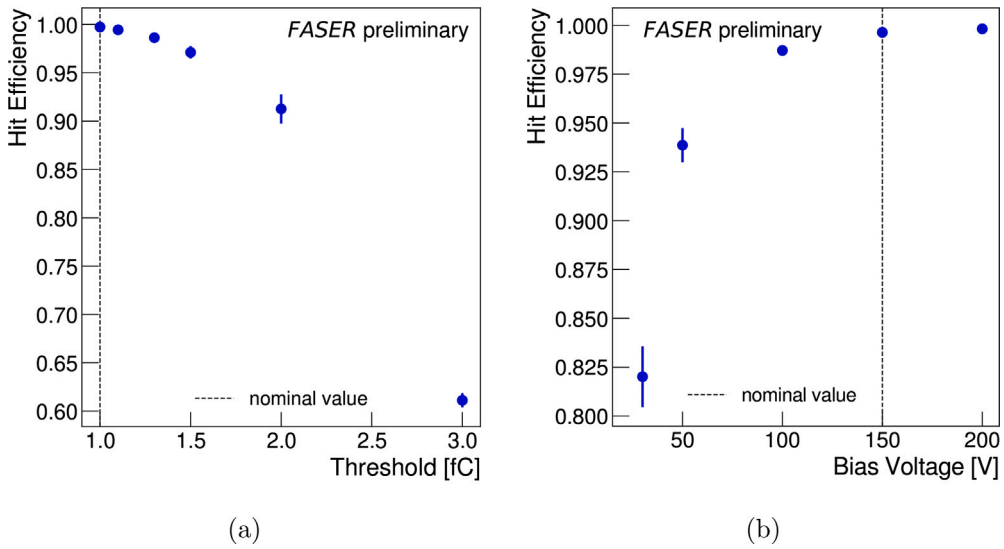

Fig. 10. Threshold and bias HV scans with early data taken at the beginning of the operation in 2022. Each scan was performed with a nominal setting except for the aimed parameter (*i.e.* threshold or bias HV). The nominal values are chosen from the regions where the hit efficiencies are sufficiently high and stable such as 1.0 fC for threshold and 150 V for Bias Voltage.

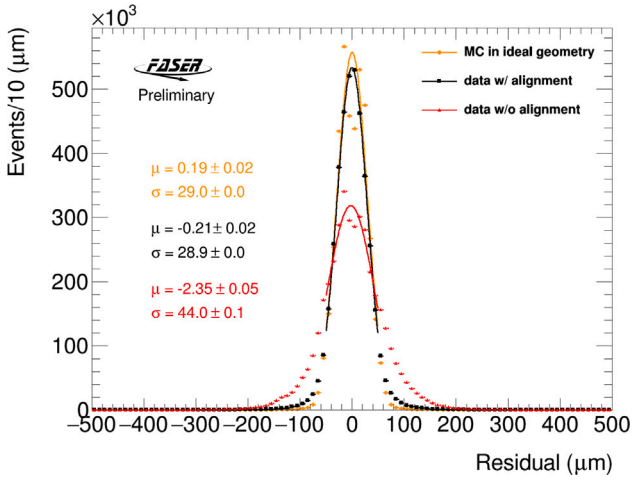

Fig. 11. Distribution of residuals from the tracks reconstructed from MC simulation in ideal geometry (orange), from data in original geometry (red), and data in aligned geometry (black) with an integrated luminosity of 596 pb^{-1}.

emulsion detector, which would allow us to identify and separately detect muons originating from ν_μ or $\bar{\nu}_\mu$, as well as potentially directly observe $\bar{\nu}_\tau$ for the first time. These studies are currently ongoing.

7. Summary

FASER, a new experiment at the LHC, started with Run 3 in 2022. Data collection is proceeding smoothly, with approximately 98% of the delivered data recorded. The FASER tracker comprises four silicon strip trackers. We have maintained consistent tracker performance over fifteen months of operation, with more than 99.7% of strips available for physics analysis. The initial alignment with collision data was performed using a simple and robust local iterative method. So far, we have achieved the expected residual values. For the future, we aim to match tracks between the IFT and FASERν to distinguish between muon neutrinos and anti-muon neutrinos, and potentially observe anti-tau neutrinos.

Declaration of competing interest

The authors declare that they have no known competing financial interests or personal relationships that could have appeared to influence the work reported in this paper.

Acknowledgments

We thank the technical and administrative staff members at all FASER institutions for their contributions to the success of the FASER project. This work was supported in part by Heising-Simons Foundation, United States Grant Nos. 2018-1135, 2019-1179, and 2020–1840, Simons Foundation, United States Grant No. 623683, U.S. National Science Foundation Grant Nos. PHY-2111427, PHY-2110929, and PHY-2110648, JSPS KAKENHI Grants Nos. JP19H01909, JP20K23373, JP20H01919, JP20K04004, and JP21H00082, BMBF Grant No. 05H20 PDRC1, DFG EXC 2121 Quantum Universe Grant No. 390833306, ERC Consolidator Grant No. 101002690, Royal Society, United Kingdom Grant No. URF R1 201519, UK Science and Technology Funding Councils Grant No. ST/ T505870/1, the National Natural Science Foundation of China, Tsinghua University Initiative Scientific Research Program, and the Swiss National Science Foundation.

References

[1] FASER Collaboration, A. Ariga, et al., Technical proposal for FASER: ForwArd search ExpeRiment at the LHC, 2018, arXiv:1812.09139 [physics.ins-det].
[2] FASER Collaboration, H. Abreu, et al., Detecting and studying high-energy collider neutrinos with FASER at the LHC, Eur. Phys. J. C 80 (1) (2020) 61, arXiv:1908.02310 [hep-ex].
[3] FASER Collaboration, H. Abreu, et al., The FASER detector, 2022, arXiv:2207.11427 [physics.ins-det].
[4] ATLAS SCT Collaboration, J.N. Jackson, The ATLAS semiconductor tracker (SCT), in: T. Ohsugi, Y. Unno, H.F.W. Sadrozinski (Eds.), Nucl. Instrum. Methods A 541 (2005) 89–95.
[5] LHCb Collaboration, LHCb Calorimeters: Technical Design Report, in: Technical Design Report LHCb, CERN, Geneva, 2000, http://cds.cern.ch/record/494264.
[6] F. Campabadal, et al., Design and performance of the ABCD3ta ASIC for readout of silicon strip detectors in the ATLAS semiconductor tracker, Nucl. Instrum. Methods A 552 (2005) 292–328.
[7] FASER Collaboration, H. Abreu, et al., The tracking detector of the FASER experiment, 2021, arXiv:2112.01116 [physics.ins-det].
[8] FASER Collaboration, Calypso software framework, https://gitlab.cern.ch/faser/calypso.
[9] X. Ai, et al., A common tracking software project, Comput. Softw. Big Sci. 6 (1) (2022) 8, arXiv:2106.13593 [physics.ins-det].
[10] V. Blobel, C. Kleinwort, A new method for the high precision alignment of track detectors, in: Conference on Advanced Statistical Techniques in Particle Physics, 2002, arXiv:hep-ex/0208021.